

UCRL- 93574  
PREPRINT

THE PRODUCTION OF  $^{38}\text{Ar}$  AND  $^{39}\text{Ar}$  BY 14-MeV  
NEUTRONS ON  $^{39}\text{K}$

K. A. Foland  
Ohio State University

R. J. Borg  
Lawrence Livermore National Laboratory

This paper was prepared for submittal to  
Nuclear Science and Engineering

November 5, 1985

Lawrence  
Livermore  
National  
Laboratory

This is a preprint of a paper intended for publication in a journal or proceedings. Since changes may be made before publication, this preprint is made available with the understanding that it will not be cited or reproduced without the permission of the author.

#### **DISCLAIMER**

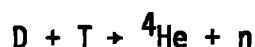
**This document was prepared as an account of work sponsored by an agency of the United States Government. Neither the United States Government nor the University of California nor any of their employees, makes any warranty, express or implied, or assumes any legal liability or responsibility for the accuracy, completeness, or usefulness of any information, apparatus, product, or process disclosed, or represents that its use would not infringe privately owned rights. Reference herein to any specific commercial products, process, or service by trade name, trademark, manufacturer, or otherwise, does not necessarily constitute or imply its endorsement, recommendation, or favoring by the United States Government or the University of California. The views and opinions of authors expressed herein do not necessarily state or reflect those of the United States Government or the University of California, and shall not be used for advertising or product endorsement purposes.**

## 1. Introduction

We have determined the cross sections for the production of  $^{38}\text{Ar}$  and  $^{39}\text{Ar}$  from the (n,n'p) and (n,p) reactions by neutrons of approximately 14 MeV incident on  $^{39}\text{K}$ . Three potassium-bearing specimens were irradiated with  $\sim 10^{17}$  neutrons, and the Ar isotopes were measured by mass spectrometry. There have been only two previous experimental measurements of these cross sections in this energy range (Borman, Jeremie, Andersson-Lindstrom, Neuert, and Pollehn<sup>1</sup>; Aleksandrov, Klochkova, and Kovrigin<sup>2</sup>). The previous measurements are in substantial disagreement with our results. The values from the three new measurements are consistent with one another, however, and indicate an increase in the cross sections for both reactions as the neutron energy increases from approximately 14.5 to 14.8 MeV.

## 2. Experimental

Samples of a natural potassium feldspar ( $\text{K}_{0.915}\text{Na}_{0.067}\text{Al}_{1.06}\text{Si}_{2.96}\text{O}_8$ ) and KBr and KI salts were irradiated with neutrons having nominal energies between 14.2 and 15.5 MeV produced by the Rotating Target Neutron Source (RTNS-II) at the Lawrence Livermore National Laboratory. The RTNS-II makes use of the reaction:



and is shown schematically in Fig. 1. Deuterons accelerated to an average energy of 400 keV bombard a titanium tritide coating on the surface of a water-cooled copper disc, which rotates at 2500 rpm in order to further dissipate the beam energy. A maximum source strength in excess of  $3 \times 10^{13}$  neutrons/cm<sup>2</sup>-s is achievable, with a distribution in mean energy varying from

14.9 MeV in the forward direction to 14.5 MeV at 60° (see Fig. 2).<sup>3</sup> We have measured the room return flux of the back-scattered forward beam at various representative locations within the target cave and estimate that it is less than  $\sim 5 \times 10^{-4}$  of the primary flux at our sample positions. The  $\sim 14$ -MeV fluence was measured by counting iron foils attached to the sample vials. The 0.835-MeV gamma emission of  $^{54}\text{Mn}$  ( $t_{1/2} = 312.5$  d) resulting from  $^{54}\text{Fe}(n,p)^{54}\text{Mn}$  is counted and used to calculate the fluence. The  $^{54}\text{Fe}$  cross sections of Greenwood et al.<sup>3</sup>, normalized to a value of 463 mb for the  $^{93}\text{Nb}(n,2n)^{92\text{m}}\text{Nb}$  reaction were used. The cumulative fluence uncertainties are estimated to be  $\pm 3\%$  for the potassium salts and  $\pm 5.5\%$  for the feldspar.

Although the deuteron beam and hence the neutron source is seldom exactly congruent with the central axis of the specimen bench, the deviation may be deduced from the relative fluences accumulated by simultaneously irradiated samples. Once the relative angle with respect to the forward direction of the beam has been established, the energy-dependent cross section for (n,p) on  $^{54}\text{Fe}$  and the mean energy of the impinging beam may be determined by applying the data shown in Fig. 2. For the three irradiated specimens, we estimate the uncertainty in mean neutron energy resulting from error in angle determination to be  $\pm 0.02$  MeV. The angles with respect to the forward-beam axis were 25° (K-feldspar), 52° (KBr), and 61° (KI).

We irradiated the samples in quartz vials; the KBr and KI salts were prepared from analytical grade reagents. The feldspar was a well-characterized natural specimen consisting of grains with an average diameter of 480  $\mu\text{m}$  and with known concentrations of K and  $^{40}\text{Ar}$ , having associated uncertainties of  $\pm 0.5$  and 1%, respectively.<sup>4</sup> The salts were prepared by melting under vacuum to form essentially air-free slugs at the bottom of their respective evacuated quartz ampoules equipped with interior break-off seals.

After irradiation, the Ar isotopes were measured by mass spectrometry at Ohio State University using a Nuclide model SGA-6-60 mass spectrometer operated in the static mode. We measured ampoule gas derived from recoil only for the KI sample. Aliquots of the irradiated material were wrapped in Al foil, introduced into a high-vacuum system, and fused in a Mo crucible by induction heating. The vacuum lines were baked at  $\sim 200^{\circ}\text{C}$  to outgas atmospheric Ar, but the gas-loaded samples were maintained at room temperature. The released gases were purified by active metal gettering. The absolute amounts of Ar were determined by isotope dilution with a high purity  $^{38}\text{Ar}$  tracer delivered by a metering system and calibrated with mineral standards of known  $^{40}\text{Ar}$  concentration.

In all mass spectrometric measurements,  $^{36}\text{Ar}$  is assumed to derive from atmospheric contamination, and the reported values have been corrected for this atmospheric argon component.<sup>5</sup> This correction is less than 0.05% to the measured salt ratio of  $^{38}\text{Ar}/^{39}\text{Ar}$  except in the case of the KI ampoule gas, where it is 4%. In the salt measurements, essentially all (96 to 99%) of the  $^{40}\text{Ar}$  may be attributed to atmospheric Ar. In the feldspar experiment, the corrections to the  $^{40}\text{Ar}/^{39}\text{Ar}$  and  $^{38}\text{Ar}/^{39}\text{Ar}$  ratios were 16 and 4%, respectively.

For the KI and KBr experiments, both isotope composition and isotope dilution measurements were required. The potassium feldspar experiment consists of a single measurement of the Ar isotopic composition. Because the concentration of  $^{40}\text{Ar}$  in this material is known, measurement of the isotopic ratios is sufficient to yield the concentrations of  $^{38}\text{Ar}$  and  $^{39}\text{Ar}$ . The cumulative uncertainties in concentration measurements are  $\pm 1.5\%$ .

In order to check the possibility of Ar loss by diffusion and/or recoil from the salts, we checked the Ar in the KI sealed breakseal ampoule. The

ampoule was attached to the vacuum line, broken open, and the Ar isotope ratios measured.. The amount of Ar measured was based only on the sensitivity of the mass spectrometer. As a further test of potential diffusive loss, an aliquot of KI was heated to 95°C for 14 hours before isotope dilution analysis.

### 3. Results

The measured Ar isotopic compositions are given in Table 1, and the Ar concentrations in Table 2. The mean neutron energies, total fluences, and calculated cross sections for the three experiments are summarized in Table 3. The various replicate measurements show good agreement.

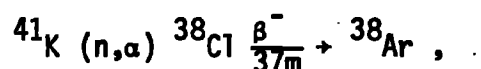
The  $^{38}\text{Ar}/^{39}\text{Ar}$  production ratio (Table 1) is about 4, ranging from 3.81 to 4.18 as the average neutron energy varies from 14.48 to 14.82 MeV. Over this energy range, the ratio of  $\sigma(n,n'p)$  to  $\sigma(n,p)$  on  $^{39}\text{K}$  thus increases by 10%, as might be anticipated. All three experiments show this systematic increase. This result follows directly from the mass spectrometry and is not affected by variations in the total fluence or absolute amounts of K or Ar, the ratio being subject to an uncertainty of only about 0.5%.

The concentrations of  $^{38}\text{Ar}$  and  $^{39}\text{Ar}$  (Table 2) are substantial and easily measured, ranging from about  $2 \times 10^{-11}$  to  $5 \times 10^{-10}$  mol/g. The measured concentrations along with K concentrations and fluences yield the apparent cross sections in Table 3. It is clear they both  $\sigma(n,p)$  and  $\sigma(n,n'p)$  increase systematically with neutron energy. The former varies from 114 to 145 mb and the latter by a larger amount, from 434 to 606 mb. The uncertainties, which are caused by imprecision in the dosimetry and concentration measurements in both cross sections, are 3.4% for the KBr and KI experiments and 5.7% for the K-feldspar experiment. The cross sections are shown graphically in Fig. 3.

Measurements of the KI ampoule gas and heated aliquot provide important information verifying the ability of the materials to quantitatively retain the produced Ar during the normal experimental procedure. Ar in the evacuated KI ampoule had the same  $^{38}\text{Ar}/^{39}\text{Ar}$  ratio as the salt; importantly, this Ar was only 0.6% of the total  $^{38}\text{Ar}$  and  $^{39}\text{Ar}$  produced and contained by the KI in the ampoule. The KI sample heated to 95°C lost only 4.5% of its Ar. These measurements indicate that loss of Ar by recoil and/or diffusion in a vacuum near room temperature does not pose a problem.

#### 4. Discussion

The method that we used has a potential problem:  $^{38}\text{Ar}$  and  $^{39}\text{Ar}$  produced from other interfering reactions could lead to an overestimation of the cross sections. However, consideration of the neutron energy spectrum, possible sample impurities, and the appropriate cross sections fails to indicate any significant interferences. The largest expected interference would derive from



for which the reported cross section is  $\sim 35$  mb. As  $^{41}\text{K}$  is but 6.73% of normal K, the contribution of  $^{38}\text{Ar}$  from this source amounts to about 0.5% of the total. All other sources are very much smaller.

Our cross sections as reported in Table 3 are in considerable disagreement with the literature values. The values given by Borman et al.<sup>1</sup> are for  $^{39}\text{K}(n,p)^{39}\text{Ar}$ ,  $\sigma(n,p) = 354 \pm 54$  mb and for  $^{39}\text{K}(n,n'p)^{38}\text{Ar}$ ,  $\sigma(n,n'p) = 186 \pm 28$  mb. Aleksandrov et al.<sup>2</sup> report  $\sigma(n,p) = 400 \pm 100$  mb and state that the cross section is decreasing with energy in the range  $E_n > 14.1$  MeV, contrary to our

observation. Not only do our absolute cross section values differ, but also our relative ratio of the two reactions is markedly different. Our value for the  $(n,p)$  reaction is much smaller, but for the  $(n,n'p)$  much larger. Assuming no significant production via other reactions, the ratio of  $\sigma(n,n'p)/\sigma(n,p)$  is equal to the measured  $^{38}\text{Ar}/^{39}\text{Ar}$ , which is the most accurate measurement reported here. Furthermore, the ratio is fairly constant, except for the systematic variation with energy, for three potassium samples of very different matrices.

Further light on the possible source of the discrepancy is apparent from the nature of the experiments by Borman et al. They determined the total emission of charged particles, i.e.,  $\alpha$  and  $p + D$ , subtracted the alpha component from the combined spectra, and calculated the relative contribution of the two reactions by classical statistical theory. It is likely that the source of error is in the deconvolution procedures applied to the combined proton spectrum. Support for this supposition is found from the agreement of the combined values of  $\sigma$  (i.e.,  $\sigma(n,p) + \sigma(n,n'p)$ ). At our lowest energy, viz. 14.48 MeV, our combined values of  $\sigma$  give 548 mb, and Borman et al. obtain essentially the same value, viz. 540 mb from their unresolved proton counting for  $\sigma(n,p) + \sigma(n,n'p)$ . Aleksandrov et al. measured the energy-dependent proton emission spectrum and again performed elementary classical calculations to separate  $(n,n'p)$  from  $(n,p)$ . It is likely that similar problems exist in their report, but there is insufficient information to quantitatively analyze their work.

As a first approximation, we have viewed the reaction cross sections in terms of average energy, even though the energy range is a few hundred keV and varies as a function of angle (see Fig. 2). Even with this limitation, there is a clear dependence of cross section on energy over the restricted neutron



energies. The values at 14.48 and 14.82 MeV are analytically distinct, indicating an increase of both  $\sigma(n,n'p)$  and  $\sigma(n,p) E_n$ , with a greater increase in the former than in the latter. It is somewhat surprising that both cross sections are increasing in this range; we plan to do further experimental and theoretical work on this aspect.

References

1. Borman, Von M., Jeremie, H., Andersson-Lindstrom, G., Neuert, H., and Pollehn, H., Z. Naturforsch. 15A, 199 (1960).
2. Aleksandrov, D. V., Klochkova, L. I., and Kovrigin, B. S., Aymnya. Enrgya. 39, 137 (1975).
3. Greenwood, L. R. (Argonne National Laboratory), Guinan, M. W. (Lawrence Livermore National Laboratory), and Kneff, D. W. (Rockwell International), DAFS Quarterly Report DOE 1 ER-0046/21, p. 15 (1985).
4. Foland, K. A., Geochim. Cosmochim. Acta 38, 151 (1974).
5. Ozima, M., and Podosek, F. A., Noble Gas Geochemistry, Cambridge Univ. Press (1983).

Table 1. Isotopic composition of Ar in irradiated specimens.

Sample	Weight (mg)	$^{40}\text{Ar}/^{39}\text{Ar}^*$	$^{38}\text{Ar}/^{39}\text{Ar}^*$
KI (ampoule gas)		5.9	3.794
KI	9.37	0.053	3.819
	8.24	0.19	3.813
	40.17	0.051	3.784
	51.92	0.217	3.818
		Average	$3.808 \pm 0.016 (\pm 0.4\%)$
KBr	8.87		4.000
	54.00		4.037
	58.43		4.036
	10.03		4.000
		Average	$4.108 \pm 0.021 (\pm 0.5\%)$
K-feldspar	25.96	916.2	4.182

\* Corrected for atmospheric Ar contamination assuming that all  $^{36}\text{Ar}$  is from atmospheric Ar with a composition of  $^{40}\text{Ar}/^{36}\text{Ar} = 295.5$  and  $^{38}\text{Ar}/^{36}\text{Ar} = 0.1180$ .

Table 2. Ar concentrations in irradiated specimens.

Sample	Weight (mg)	$^{39}\text{Ar}$ (mol/g)	$^{38}\text{Ar}$ (mol/g)	$^{39}\text{Ar}/^{39}\text{K}^*$ (mol/mol)	$^{38}\text{Ar}/^{39}\text{Ar}^*$ (mol/mol)
KI (ampoule gas)		$4.2 \times 10^{-13}$	$1.6 \times 10^{-12}$	moles total	
KI	66.47	$5.503 \times 10^{-11}$	$2.095 \times 10^{-10}$		
	77.61	$5.427 \times 10^{-11}$	$2.066 \times 10^{-10}$		
	Average	$5.465 \times 10^{-11}$	$2.081 \times 10^{-10}$	$9.730 \times 10^{-9}$	$3.705 \times 10^{-8}$
KBr	63.07	$1.355 \times 10^{-10}$	$5.445 \times 10^{-10}$		
	68.27	$1.373 \times 10^{-10}$	$5.517 \times 10^{-10}$		
	Average	$1.364 \times 10^{-10}$	$5.481 \times 10^{-10}$	$1.740 \times 10^{-8}$	$6.993 \times 10^{-8}$
KI**	87.74	$5.217 \times 10^{-11}$	$1.987 \times 10^{-10}$		
K-feldspar***	25.96	$2.62 \times 10^{-11}$	$1.10 \times 10^{-10}$	$8.80 \times 10^{-9}$	$3.64 \times 10^{-8}$

\* Calculated assuming stoichiometric salt and feldspar with  $3.23 \times 10^{-3}$  mol K/g (Foland<sup>4</sup>), and  $^{39}\text{K} = 93.258$  atom % of normal K.

\*\* Aliquot heated at 95°C for 14 h.

\*\*\* Ar concentrations from the isotope ratios and a feldspar  $^{40}\text{Ar}$  concentration of  $2.40 \times 10^{-8}$  mol/g (Foland<sup>4</sup>).

Table 3. Summary of the measured cross sections for the three experiments.

$E_n$ (average) (MeV)	Total $\phi$	Expt.	$\sigma_{n,p}$ (mb)	$\sigma_{n,n'p}$ (mb)	$\frac{\sigma_{n,n'p}}{\sigma_{n,p}}$
14.48	$8.53 \times 10^{16}$	KI	114	434	3.81
14.58	$1.40 \times 10^{17}$	KBr	125	500	4.02
14.82	$6.01 \times 10^{16}$	K-feldspar	145	606	4.18

Figure Captions

Fig. 1. Schematic of section of target system of RTNS-II. The shaded area shows the portion that rotates at 2500 rpm. The angle between the axis of rotation and the deuteron beam is slowly varied to use the entire tritium-coated band on the inside of the target. The neutron source remains stationary in the room. To acquire maximum neutron flux, samples are placed as close as reasonable to the exterior surface of the spinning target.

Fig. 2. Neutron energy spectra for various angles of RTNS-II.

Fig. 3. Measured cross sections as a function of average neutron energy.

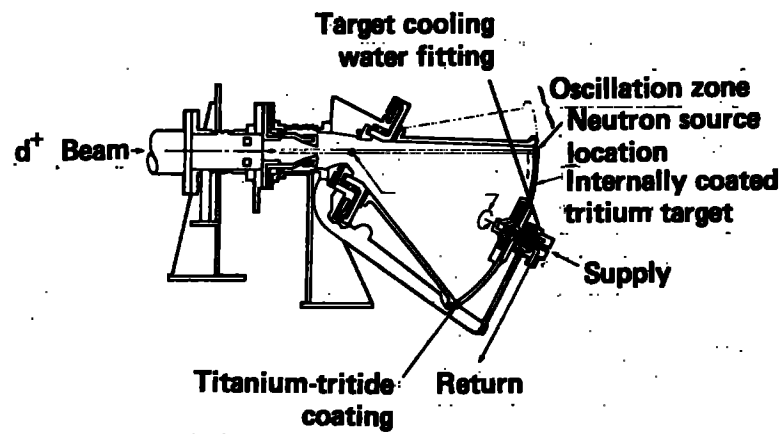


FIGURE 1

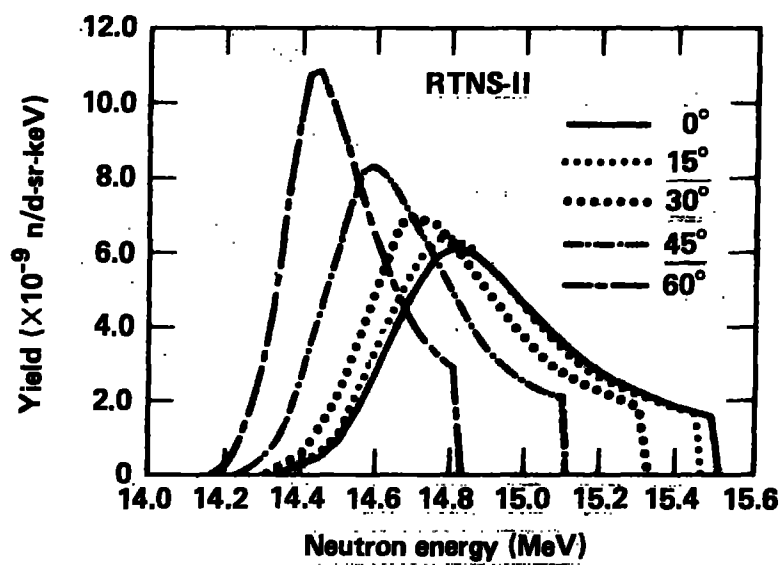


FIGURE 2



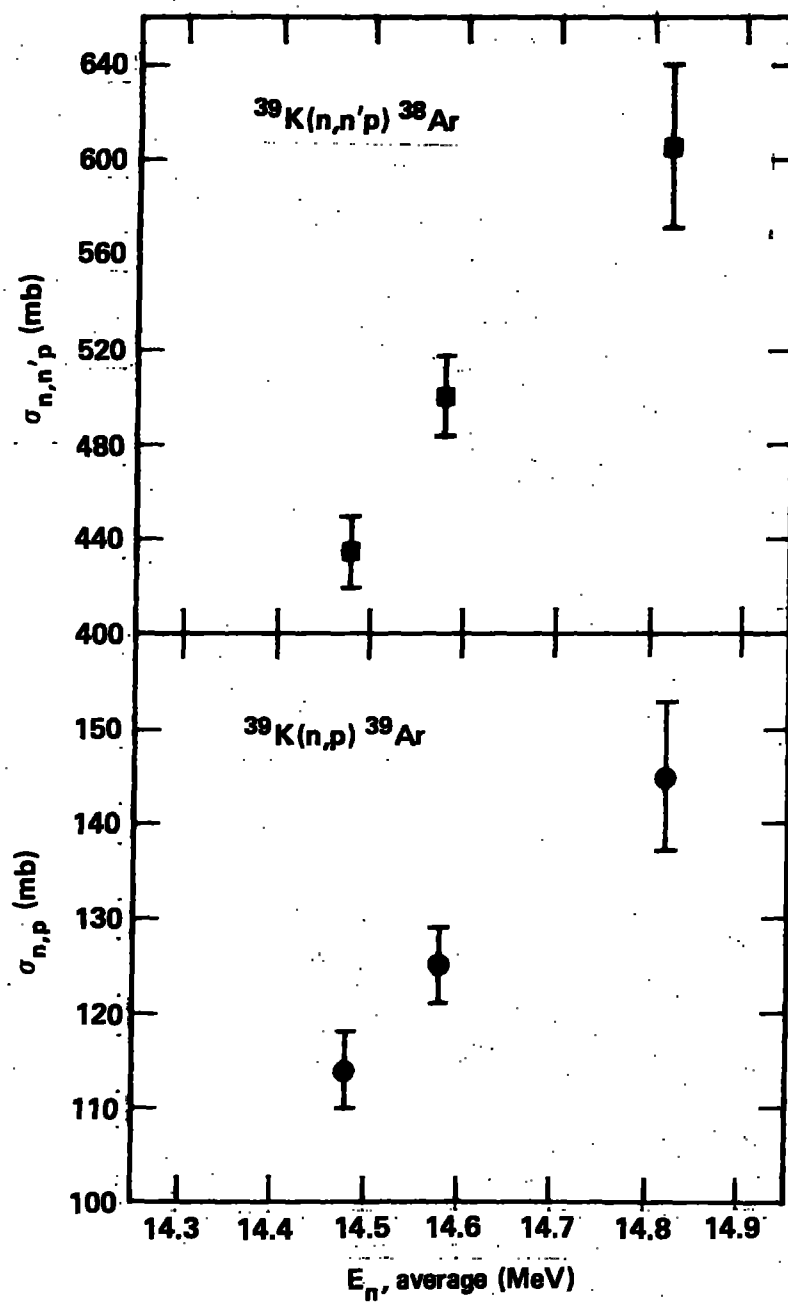


FIGURE 3